



THE 15th CHESAPEAKE SAILING YACHT SYMPOSIUM

An experimental investigation of slamming on ocean racing yachts.

Paolo Manganeli, Ship Science, School of Engineering Sciences, Southampton, UK

Philip A. Wilson, Ship Science, School of Engineering Sciences, Southampton, UK

ABSTRACT

Groupe Finot Naval Architects and the School of Engineering Sciences, Ship Science of the University of Southampton have started a joint research project to carry out an experimental investigation concerning the effects of slamming on offshore sailing yachts.

A reliable autonomous data acquisition system was designed that allowed measurements to be taken during long offshore races. The details of the design and implementation of this system are presented together with some sample results from the first measurement campaigns.

NOTATION

| | |
|------------|--|
| A_{cg} | Acceleration at the centre of gravity |
| B_{MAX} | Maximum beam |
| B_{WL} | Beam at waterline |
| DSA | Downwind sail area |
| $H_{1/3}$ | Significant wave height |
| LCG | Longitudinal centre of gravity |
| L_{OA} | Length overall |
| L_{WL} | Length at waterline |
| nre | Normalised rms error |
| T | Draft |
| TWA | True wind angle |
| USA | Upwind sail area |
| Δ | Displacement |
| ϵ | Angle between the boat vertical axis and the direction of acceleration |
| ∇ | Volume displacement |

INTRODUCTION

The lighter the structure the higher the loads. This is one of the most interesting (and difficult) challenges in the structural design of racing yachts. In reality, with all the other characteristics of the boat remaining the same, lighter structures allow higher ballast-to-weight ratios and

thus higher righting moments. These in turn translate into larger sideforces, larger driving forces and better speed through the water or, in other words, larger aerodynamic and hydrodynamic loads.

This challenge has been met in the past thanks to constant progress in material properties and more and more efficient design. However, the challenge is always open and lighter structures and faster boats are still to be built. One of the conditions to carry structural optimisation to a further stage is certainly a better definition of the external loads. In this respect, while structural analysis of sailing yachts has relied for years on a static or quasi-static approach, there is an increasing necessity for trying to evaluate dynamic loads and their effect in a more precise way.

High hydrodynamic loads act during a slam in the form of a localised pressure pulse rapidly travelling over a limited part of the hull. Typically, as the forward sections of the boat strike the water surface, the hull panels in the slamming area are affected by a highly non-uniform pressure distribution with peak values that can reach a thousand times the order of magnitude of the hydrostatic pressure. These peaks only act on a very limited area (smaller than the average panel size) and for a very short time (typical recorded pulse durations are between 15 and 50 ms).

For design purposes, the tendency has always been to represent these loads by an equivalent static pressure uniformly distributed over the panels. When the duration of the pressure pulse is considerably longer than the natural periods of the panels, this pressure can simply be taken as the spatial average of the real hydrodynamic load. Alternatively, if the panel is expected to show a non negligible dynamic response, the equivalent pressure would be defined as that pressure which, if applied to the panel, will result in the same deformation and same maximum stress produced by the actual loading (Heller and Jasper, 1961; Allen and Jones, 1978).

Most of the published research about slamming on sailing yachts has concentrated on the definition of suitable

values for an equivalent pressure. Several authors have contributed with theoretical and experimental investigations on this subject. Joubert (1982), Brown, Joubert and Yan Ping (1996) and Brown, Wraith and Joubert (1999) have carried out an extensive analysis of local pressure loads on hull plating and the associated structural response. They concluded in most instances that the rules in the American Bureau of Shipping "Guide for building and classing Offshore Racing Yachts" might lead to inadequate scantlings.

Reichard (1984) and Hentinen and Holm (1994), carried out some full-scale measurements by instrumenting sailing boats with pressure transducers. The latter also deduced that actual pressures are higher than the ones recommended by the ABS guide and that the unaccounted nonlinear mechanical behaviour of the hull panels combined with design safety-factors would explain the relative absence of damage on most sailing vessels. Their conclusion then was that "*there is a lot to learn about slamming loads, and the mechanisms of the structures are yet by no means fully understood*".

Indeed the question about the correct definition of design pressures for modern sailing yachts remains an open problem. Brown et al. (1999) suggest that, because every impact produces a different impact pressure, what is needed is an estimate of worst case loading. This would certainly be valuable information for design purposes, but it would not be sufficient. In fact if slamming loads are to produce a structural failure, it is more likely to happen because of fatigue rather than because of maximum stress exceedance. For example, this was probably the case with the numerous sandwich core failures observed at the end of leg 5 of the 1993-94 Whitbread race: as Bowler commented (Jeffrey, 1998) failures only started to appear on yachts after they had sailed 20000 miles and most of them had already survived conditions similar to or heavier than those encountered during leg 5 without damage. Hence, ideally materials and scantling definition should also take into account non-maximum slamming loads and their frequency of occurrence.

EXPERIMENTAL INVESTIGATION

The investigation focused on Open'50 and Open'60 class boats. These are ocean racing yachts designed primarily for single-handed sailing. Several aspects make them very suitable for this type of study: their high beam-to-length ratio and relatively low equivalent deadrise angles favour large impact loads. Their steering relies for more than 95% of the time on auto-pilot systems: such devices, while trying to keep a constant heading or a constant apparent wind angle, are "blind" with respect to the incoming waves and do not take any action to avoid or reduce slamming. Finally, Open'60 are currently among the fastest sailing monohulls, capable of sustaining steady speeds of more than 20 knots while sailing in rough seas. In choosing a way of investigating slamming loads, a solution had to be determined that was compatible with this type of boat. In addition, it was considered that

measurements should be taken during races as in these conditions voluntary speed reduction is minimal and the highest loads are likely to appear. This would sensibly narrow down the possible choices regarding the sensors and the data acquisition system to be used. Pressure transducers, although being the only devices that allow direct measurement of hydrodynamic loads, were ruled out. There were two main reasons for this choice: firstly, to resolve the pressure distribution over the hull and its evolution in time, a relatively dense array of sensors must be employed (Allen and Jones, 1978, Rosen and Garme, 1999). This, together with the necessity of sampling the signals at high frequencies (i.e. more than 1 KHz), involves using data acquisition systems that are capable of processing and storing large quantities of data, but are not suitable to be installed on board an offshore sailing yacht during a race. Secondly, from a purely practical point of view, pressure transducers potentially affect the water-tightness of the boat, as they need to be fitted through the hull and no skipper would accept it.

Using displacement transducers and strain gauges was considered as an alternative. These devices allow the measurement of the structural deformation that is induced by slamming loads. Displacement transducers, in particular, may give an indication of the inward deflection of hull panels whilst strain gauges would provide useful data about the relative amount of bending and membrane deformation. Unfortunately, both type of sensors would be difficult to fit on our test boats and their use appeared incompatible with long-term unattended measurement campaigns.

The best solution was to use accelerometers. If they are mounted on the primary structure (bulkheads and girders) they allow rigid-body accelerations to be recorded and the global dynamic structural behaviour to be identified while, if fixed directly onto the hull plating and on secondary reinforcements (i.e. stringers and frames), they give an indication about the local structural response. Indeed, through double integration of their signal in the time domain, it is also possible to calculate their displacement and hence amplitudes of rigid-body motion and of structural deformation.

It is arguable that the magnitude of the rigid body acceleration following an impact is proportional to the hydrodynamic load acting on the hull. This is one of the main conclusions of the theory of Heller and Jasper (1961), from which formulae for the definition of design pressures are generally derived (see DNV Tentative Rules for classification of High Speed and Light craft, 1991, A.B.S. Rules for building and classing High Speed Craft, 1997, and Draft ISO Standard 12215 for Small Craft Hull Construction/Scantlings, 2000). However, their model relied on the assumptions that "*the time variation of the load has only a small amount of high-frequency content*" and that the hull acts "*nearly*" as a rigid body during the water impact. Although using accelerometers would not allow us to verify the validity of the first assumption, it would give us a good indication of the relative amount of energy present in the flexible modes or, in other words, of

how accurate it is to consider the boat “rigid” through the impact. The next section will concentrate on the details of how these sensors and the data acquisition system were set up.

Experimental setup

For measurements during long offshore races, seven accelerometers and a programmable data-logging unit were used. The position and the orientation of the sensitive axes of the accelerometers are shown in figure 1. Two sensors were mounted on the collision bulkhead (which is approximately at 13% of L_{OA} on Open’50s and at 5% of L_{OA} on Open 60’s) measuring acceleration along the Y and Z axes (respectively 1 and 2 in the figure). Four were fixed to the bulkhead closest to the centre of gravity (approximately at 50 % of L_{OA}), two on the sides (3 and 4) measuring acceleration along the Z axis and two on the centreline measuring along the X and Y axes (6 and 5). Finally, one accelerometer was mounted on a bulkhead in the aft area (approximately at 90% of L_{OA}) measuring along the Z axis (7). Although six accelerometers would be sufficient to measure the six components of rigid-body motion, seven were used in order to have some redundancy on the measurement of heave and pitch acceleration and to identify the amplitude of longitudinal bending vibration.

For two reasons *IC Sensors 3140* accelerometers were chosen: internal signal amplification allowed a very good signal-to-noise ratio to be achieved despite the long lengths of cable, while built-in temperature compensation guaranteed very small drift over time (typically less than $\pm 0.01g$), avoiding the need for constant recalibration. All had a $\pm 10g$ measurement range except for 5 and 6 where a $\pm 5g$ range was chosen to give a better resolution. Their linear bandwidth extends from 0Hz to 500Hz.

With respect to rigid-body motion measurement, the use of inertial measurement units was considered: these devices generally include three angular rate sensors and three accelerometers to measure oscillatory motion in six degrees of freedom. The main advantage over strap-down accelerometer systems is that one less stage of integration is needed to calculate angular motions, so dynamic

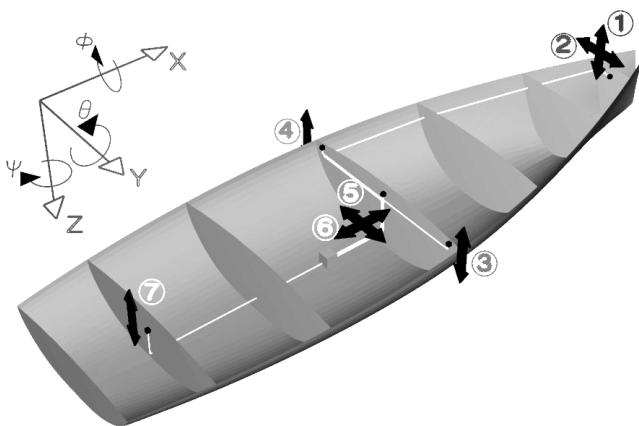


Fig. 1 Position and sensitive axes of the accelerometers

accuracy is better. Besides, their reliability and their weight have been sensibly improved in the recent years thanks to the introduction of vibrating quartz and laser ring gyros in place of traditional spinning mass units. However, cost and power consumption are still considerably higher than those of systems using only accelerometers, and these factors were of primary importance for us.

For the data acquisition, a customised logging unit supplied by the Cranfield Impact Centre was used. Up to eight analogue signals could be logged through an A/D converter equipped with programmable filters. Data from the boat instruments could equally be recorded through a standard NMEA interface. The maximum allowed sampling frequency per channel was 2 KHz.

The unit was programmed to perform all the following tasks at the same time:

Logbook acquisition: a single sample of boat speed, boat heading, true wind speed, true wind angle and GPS position was stored at regular intervals (typically 20 seconds). This provided a useful reference about the sailing conditions.

Short time-histories recording: whenever the vertical acceleration at the bow or at the centre of gravity exceeded preset threshold values, a short time-history of all the accelerometer signals was recorded. In particular, the logging unit had a circular memory buffer that allowed it to store not only the data following a triggering event, but also those that preceded it. Hence, typically, the five seconds preceding a “slam” and the five following are recorded. The analogue channels are normally sampled at 100Hz while a single sample of boat speed, true wind angle, true wind speed and GPS position is attached to the time-history. The unit has a permanent internal clock so that every acquisition is time-stamped.

Data reduction: multi-dimensional histograms were continuously built up. Figure 2 shows an example: peak values of acceleration at the centre of gravity (A_{cg}) are counted and separated in different bins depending on their magnitude and on the value of the apparent wind angle (TWA) at the time of impact. Along the axes are shown the central values of each bin. Note that the graph in this example was built over a period of several days where downwind sailing conditions were predominant. This explains the large number of impacts in the 70 –90 degrees category. Similar histograms were recorded relating acceleration at the centre of gravity and at the bow to boat speed and to wind speed.

The priorities in the design of the data acquisition system were to minimise weight and power consumption, and to maximise ruggedness and autonomy. As a result the logging unit only weighed 750g and it absorbed a maximum current of 225mA from a 12V supply. All the parameters of the acquisition were programmed before the boat would leave port: when sailing, the acquisition would stop only in case of a major power supply failure (i.e. voltage of the batteries dropping below 7V) and it would resume as soon as the supply was re-established. Data were constantly saved to permanent memory and they

were retrieved when the boat arrived to port. No user intervention was ever required during the voyage. The whole system was waterproof and particular attention was paid to protecting every component from electro-magnetic interference.

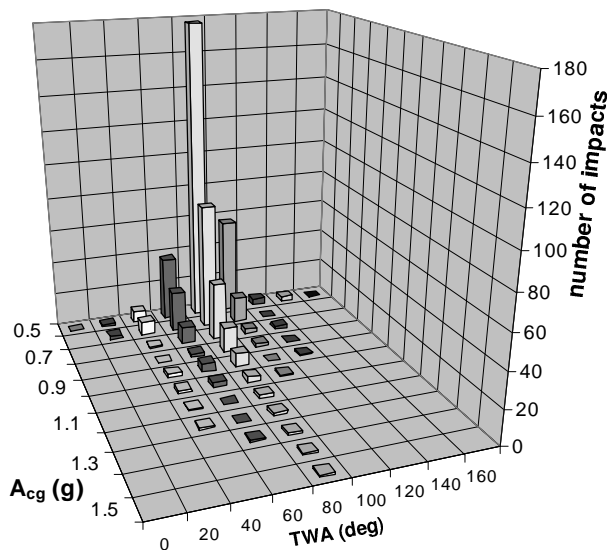


Fig. 2 Bi-dimensional histogram of A_{cg} and TWA

MOTION MEASUREMENT

All DC type accelerometers respond to the component of the acceleration of gravity aligned with their sensitive axis, thus before the measurements can be examined, they must be corrected for the effects of heel and trim changes. This can be done by implementing an iterative analysis procedure proposed by Miles (1986). The technique uses integration in the frequency domain to solve the full non-linear differential equations for the linear and angular displacements.

The method was validated by applying it to a model running in a towing tank. Accelerometers were fitted on the model in the same positions where they are on a real boat. The longitudinal separation between accelerometers 1 and 7 was 1440mm; the lateral separation between 3 and 4 was 470 mm. The model was towed at a fixed speed in regular and irregular waves. It was free to heave and pitch and constrained in sway, surge, roll and yaw. Heave and pitch displacements obtained from the accelerometer measurements were compared with those given by a displacement transducer and by a potentiometer on the towing post. Figure 4 shows a typical example of this comparison. Tests were made at four different angles of heel to assess the possible presence of coupling in the measurements of heave and sway. As shown in figure 3 the normalised rms errors expectedly increased with the heel angle. The error on heave measurement was less than 6% even at large angles, while the error on pitch measurement remained under 4%. Finally measurements of sway roll and yaw from the accelerometers, gave negligible values, which were well within the play in the

towing structure.

These results proved the analysis procedure to be very accurate and gave us confidence to apply it to full-scale measurements.

DETERMINATION OF ENCOUNTERED SEAWAY

Among all the factors that determine the magnitude and the frequency of occurrence of slamming, sea state is certainly one of the most relevant. In order to give a better interpretation of our results, it was then extremely important to obtain information about the encountered seaway. Normally, during seakeeping tests, wave buoys are used to measure the main wave characteristics. Otherwise, on-board wave radars have proved to give good estimates of significant wave height and main period in most cases. None of these devices however, can be used for long-term measurement campaigns, so an alternative source of information had to be defined. Through the Southampton Oceanographic Centre, it was possible to access measurements of significant wave height and zero up-crossing period taken by satellite altimeters. Data about local wave height and period were equally provided by a computational wave model based on winds and currents and run by the Ocean Modelling Branch (OMB) of the U.S. National Oceanic and Atmospheric Administration (NOAA). Satellite altimeters are regarded as the most accurate source of information, however, as they orbit around the globe, their ground footprint is very often too distant from the actual position of the boat to give useful information. On the other hand, computational models can be less reliable, but they always provide values very close to the position of the boat (typical data grid densities are 1 deg latitude by 1 deg longitude). Whenever it was possible to compare them the two sources were generally in good agreement: figure 5 illustrates the statistical distribution of the difference between the measurements of $H_{1/3}$ by the two methods over the month of March 2000 (when the first campaign

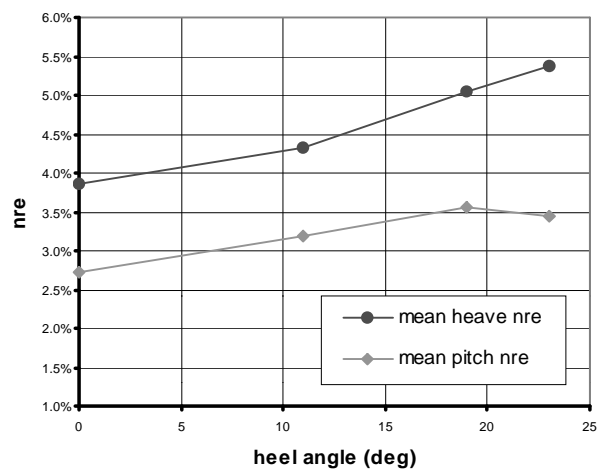


Fig. 3 Normalised RMS errors between real and estimated motion

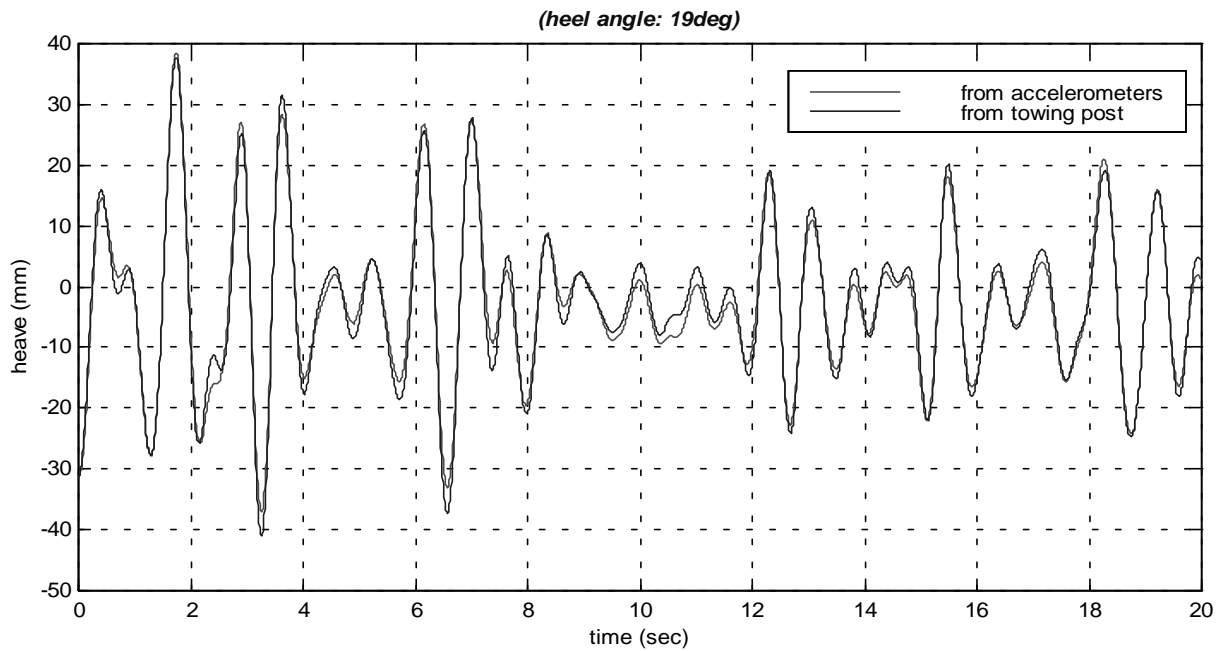


Fig. 4 Comparison of heave measurements

was carried out). These data are closely matched by a gaussian distribution with a 0.057 average and 0.134 standard deviation, suggesting that the value given by the computational model approximates the satellite observation with better than 19% accuracy in 70% of the cases.

In view of these results, it seemed justified to use data from the computational wave model in our analysis and integrate them with satellite altimeter measurements whenever these were available.

SAMPLE RESULTS FROM THE FIRST MEASUREMENT CAMPAIGNS

At the time of writing, three main measurement campaigns have been carried out, two during delivery trips across the

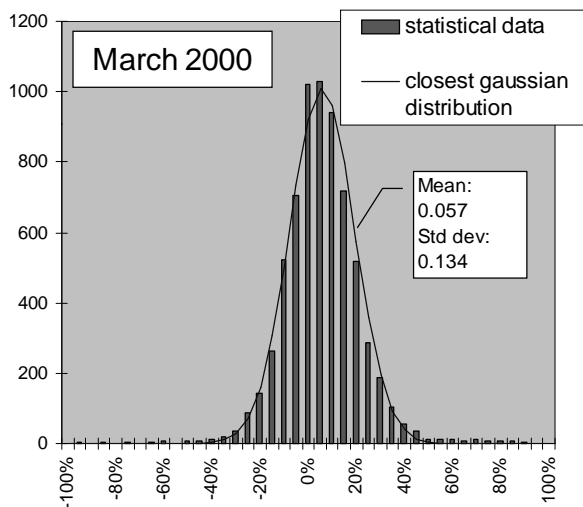


Fig. 5 Percentage difference between significant wave heights estimated by computational model and measured by satellite altimeter.

Atlantic Ocean on Open'60s and one during a single-handed transatlantic race on an Open'50. The main characteristics of these boats are listed in table 1. Although when not racing, the constraints about weight and power consumption are less strict, the system has always been used in its "racing" configuration i.e. with only seven accelerometers. The reason for this was the necessity to test the system thoroughly in view of its use during the Vendee Globe Challenge 2000, a non-stop round-the-world race. So far, recordings have been taken over 51 days and 9650 sailed miles.

During our first campaign across the Atlantic, one of the authors could be on board: this was particularly useful, not only to identify and solve initial problems, but also to perform several different types of acquisition during the same trip. Typically, the two main problems in the beginning were to identify suitable triggering conditions for the time-history recordings and cut-off frequencies for the low-pass filters.

| | Gartmore | Group4 | sailthatdream.com |
|-----------------|---------------------|---------------------|---------------------|
| Class | Open'60 | Open'60 | Open'50 |
| L_{OA} | 18.28m | 18.28m | 15.24m |
| B_{MAX} | 5.60m | 5.60m | 4.95m |
| L_{WL} | 18.28m | 18.28m | 15.24m |
| B_{WL} | 3.50m | 3.50m | 2.93m |
| T | 4.5m | 4.5m | 4.12m |
| Δ | 9.4t | 9.2t | 5.2t |
| USA | 280m ² | 246m ² | 192m ² |
| DSA | 500m ² | 500m ² | 345m ² |
| $L/V^{1/3}$ | 8.72 | 9 | 8.8 |
| Material (hull) | Carbon fibre /nomex | Carbon fibre /nomex | Carbon fibre /nomex |

Table 1 Main boat characteristics

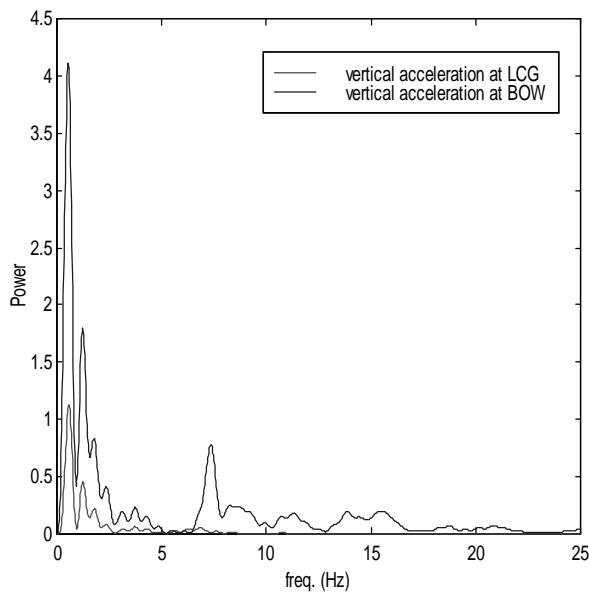


Fig. 6a Typical power spectra of signals from accelerometers mounted near the bow and near the LCG.

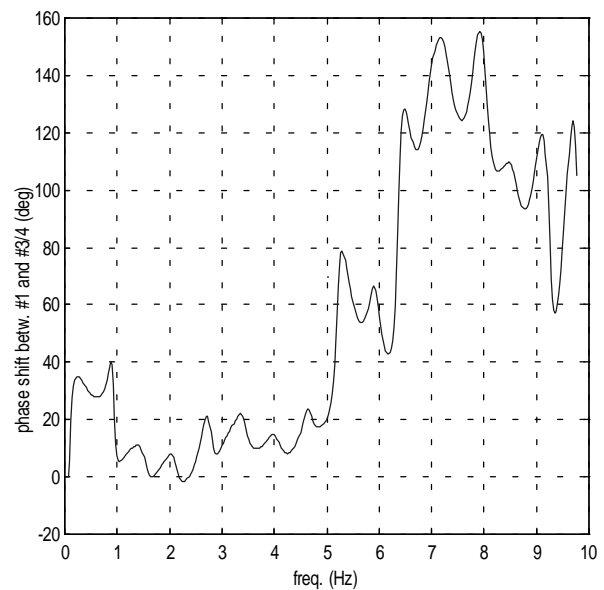


Fig. 6b Phase difference between the signals of accelerometers mounted at the bow and close to LCG.

Before being acquired, all the signals were low-pass filtered to avoid aliasing: initially the cut-off frequency was set to 40 Hz and the sampling frequency to 200Hz in order to check the frequency content of the signals. Figure 6a shows typical frequency spectra of the signals from accelerometers 1, 3 and 4. Most of the power is in the 0-1Hz band, corresponding to the wave encounter frequencies. Minor peaks can be distinguished particularly on the bow accelerometer at 7Hz, 12Hz, and 15 Hz: these correspond to resonance of flexible modes. In order to distinguish the frequency components of the signal related to rigid-body motion from those related to structural deformation, the phase of the signals were analysed. Figure 6b shows an example of the difference between the phase of the signals from accelerometers 1, 3 and 4. Non-zero values in the 0-1 Hz band are produced by the combination of heave and pitch rigid-body modes, while phase differences of up to 160 deg in the frequency range above 5 Hz indicate structural deformation (in this case longitudinal bending vibration). This pattern was consistent through all the measurements on Open'60s and Open'50s, with slightly higher resonant frequencies in the latter case. It was then concluded that most of the energy associated with flexible modes of the hull would be in the frequency band above 5Hz and 6Hz respectively for Open'60s and for Open'50s, and that the rigid-body component of the signals would be identified by low-pass filtering with a 5Hz cut-off frequency.

Recorded rigid-body accelerations

The highest accelerations were measured on the Open'50 Sailthatdream.com during the Europe1 Newman transatlantic race. As shown by figure 7, upwind sailing conditions were predominant in this event. The maximum recorded values of acceleration were 1.72g at the centre of

gravity and 5.31g at the bow. These occurred while the boat was beating at approximately 8 knots in 5.1 metres estimated significant wave height. In the same circumstances several impacts produced accelerations greater than 1.5g at the centre of gravity and than 4g at the bow. Table 2 was constructed from the recordings made over the whole race: it indicates that, at closer wind angles, the average magnitude of the accelerations increased almost linearly with the wave height. Conversely, at all true wind angles, the frequency of the impacts appeared to be higher for significant wave heights between two and three metres. This is most likely to be explained by the wave encounter frequency being higher in this range of significant wave heights. The data in table 2 also show that no significant acceleration was recorded while sailing at true wind angles greater than 120 degrees, however the number of hours spent at this heading was too small to allow any conclusion to be drawn. In fact, the third measurement campaign proved that substantial accelerations can be experienced when sailing downwind. Here several severe "slams" were recorded at true wind angles higher than 120 degrees when wave height was greater than 4m. In particular, the highest recorded acceleration was 1.22g at the centre of gravity and it occurred while the boat was sailing at 22 knots with a true wind angle of 133 degrees.

At this point, it should be noted that, in several impacts, the transverse acceleration component was found to be of a similar magnitude to the vertical one, therefore suggesting that a considerable part of the hydrodynamic load was born by the hull topsides. As shown in figure 8 and 9, the actual orientation of the maximum acceleration expectedly depended both on the heel angle and on the true wind angle (which often corresponds to the heading relative to the waves).

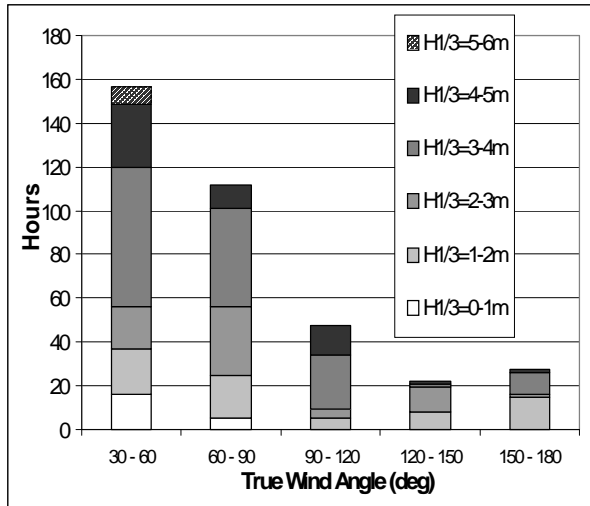


Fig.7 Distribution of time spent sailing at different true wind angles and in different significant wave heights

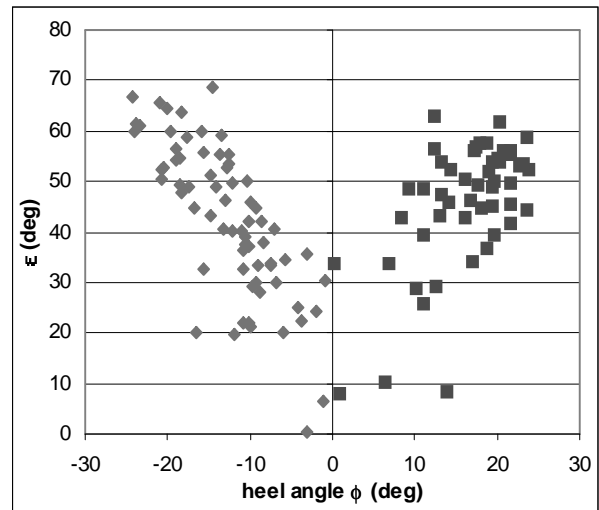


Fig.8 Measured angles of the acceleration vector at the bow relative to the vessel-related vertical axis as a function of heel angle.

| | TWA | | | | |
|---------------------------|-----------------|-----------------|-----------------|-----------|-----------|
| | 30 - 60 | 60 - 90 | 90 - 120 | 120 - 150 | 150 - 180 |
| $H_{1/3} = 0 - 1\text{m}$ | 0 | 0 | | | |
| $H_{1/3} = 1 - 2\text{m}$ | 0.33/h 0.73g | 0.36/h 1.13g | 0 | 0 | 0 |
| $H_{1/3} = 2 - 3\text{m}$ | 1.93/h 0.82g | 1.87/h 0.86g | 1.67/h 0.84g | 0 | 0 |
| $H_{1/3} = 3 - 4\text{m}$ | 0.89/h 0.98g | 0.09/h 0.79g | 0 | 0 | 0 |
| $H_{1/3} = 4 - 5\text{m}$ | 0.52/h 1.03g | 0 | 0 | 0 | |
| $H_{1/3} = 5 - 6\text{m}$ | 0 | | | | |

Table 2 Example of impact characteristics as a function of true wind angle and significant wave height. The value in the top-left corner of each cell indicates the average number of impacts per hour that produce an acceleration greater than 2g at the bow. A value equal to 0 means that the 2g threshold was never exceeded. The number in the bottom-right corner represents the corresponding average acceleration at the centre of gravity. Cells are empty where the conditions were out of the spectrum met during the measurement campaign.

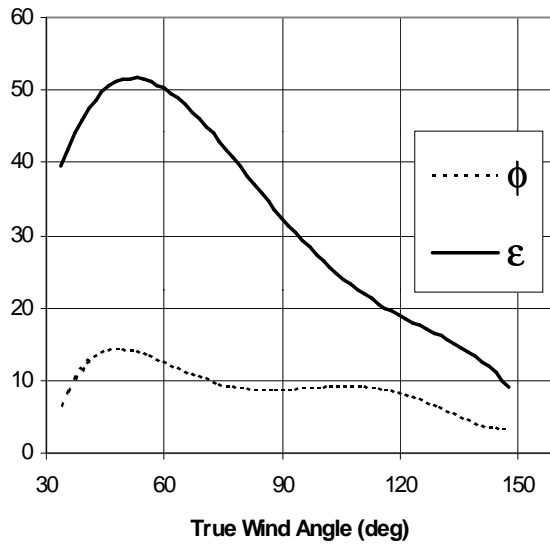


Fig.9 Example of relation between true wind angle, angle of acceleration at the bow (ϵ) and heel angle (ϕ). The curves represent the moving average of the measured values.

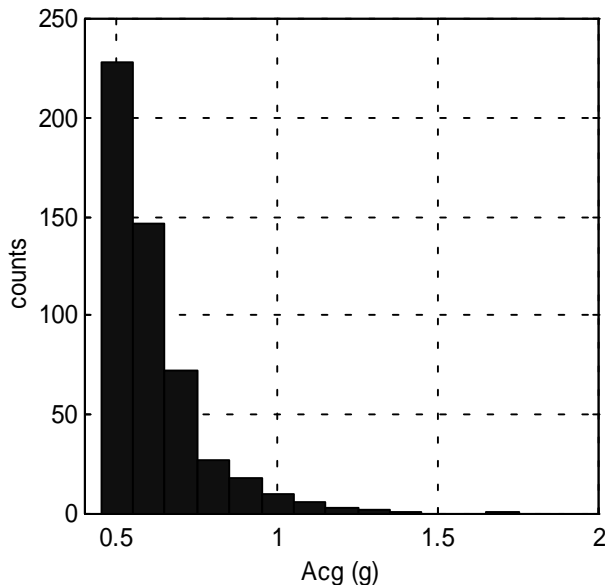


Fig.10 Example of relative frequency of acceleration at the centre of gravity.

Maximum values of rigid-body accelerations from each measurement campaign were analysed statistically. Figure 10 shows an example of the histograms of the peak accelerations at the centre of gravity, built during the measurement campaigns. By analysing these data in terms of cumulative distributions, it was observed that the recordings always matched very closely a Weibull probability distribution function. This had to be written in

the form:

$$F_X(x) = 1 - e^{-\left(\frac{x-x_0}{k}\right)^r}$$

where x_0 was equal to 0.5g, the central value of the smallest bin in the recorded histograms. Parameters “k” and “r” were estimated by a linear least squares method. Figure 11 shows an example of the results from the tests on an Open’60. With k and r known, the probability of accelerations exceeding a given value x could be calculated as the joint probability $P_1[A_{cg} \geq 0.5g] \cdot P_2[A_{cg} > x]$ where:

$$P_1 = \frac{2\pi \cdot N_A}{T_R \cdot \bar{\omega}_e} \quad \text{and}$$

$$P_2 = e^{-\left(\frac{x-x_0}{k}\right)^r}$$

with:

N_A : number of counted accelerations exceeding 0.5g

$\bar{\omega}_e$: average encounter frequency over the recording period (which could be estimated from acquired time histories)

T_R : recording time.

Similarly, the average of the $1/N^{\text{th}}$ highest accelerations could be obtained as:

$$\bar{x}_{\frac{1}{N}} = k \cdot M \cdot \left[\frac{(\ln M)^{1/r}}{M} + \frac{1}{r} \cdot \Gamma(1/r) \cdot (1 - P(1/r, \ln M)) \right]$$

with: $M = N/P_1 = N \cdot \frac{T_R \cdot \bar{\omega}_e}{2\pi \cdot N_A}$

and Γ and P respectively the complete and incomplete Gamma functions.

CONCLUSIONS

A data acquisition system has been designed and implemented to study slamming on ocean sailing yachts. Slamming events have been characterised by measuring the rigid-body accelerations and the vibration that they induce in the structure. Rigid-body accelerations have been measured in six degrees of freedom by means of seven strap-down accelerometers. An iterative analysis procedure that allows the calculation of linear and angular displacements from acceleration recordings has been experimentally validated.

Statistical analysis of the results from long measurement campaigns has shown that peak values of acceleration always tend to follow a Weibull probability distribution function. A method has been outlined that allows the calculation of the probability of exceedance of given thresholds and of averages of highest values.

Time histories of the accelerometer signals recorded

during slams have suggested that considerable bending and torsional vibrations are initiated by slamming. Further measurement campaigns are planned in which a larger number of sensors will be used to get a better definition of modal shapes and amplitudes.

ACKNOWLEDGEMENTS

This work would not have been possible without the support of Jean-Marie Finot and of all the people at Groupe Finot Naval Architects: to them we wish to express our deepest gratitude.

We would also like to thank the Wolfson Unit for Marine Technology and Industrial Aeronautics for their assistance throughout the project.

Special thanks go to Josh Hall, Alex Thomson, Mike Golding and Bernard Gallay for letting us install our equipment on their boats.

REFERENCES

Heller, S.R., Jasper, N.H., "On the structural design of planing craft", Transactions of the Royal Institution of Naval Architects, Vol.103, 1961, pp 49-65.

Allen, R.G., Jones, R.R., "A simplified method for determining structural design-limit pressures on high performance marine vehicles", American Institute of Aeronautics and Astronautics, 1978.

Joubert, P.N., "Strength of Bottom Plating of Yachts", Journal of Ship Research, Vol.26, No.1, March 1982, pp.45-49.

Brown, K.C., Joubert, P.N., Ping Yan, "Tests on Yacht Hull Plating", Marine Technology, Vol.33, No.2, April 1996, pp.130-140.

Brown, K.C., Wraith, R.G., Joubert, P.N., "Local Pressure on Hull Plating Due to Slamming", 5th International Conference on Fast Sea Transportation, Seattle, September 1999.

Reichard, R.P., "The Structural Response of Small Craft to Dynamic Loading", Proceedings of the Fourteenth AIAA Symposium on the Aero/Hydrodynamics of Sailing, Vol.30, Lay Beach, November 1984.

Hentinen, M., Holm, G., "Load measurement on the 9.4m sailing yacht 'Sail Lab'", 13th International Symposium on Yacht Design and Yacht Construction, Amsterdam, Nov.1994.

Jeffrey, T., "Core of the problems", Yachting World, No.146, July 1994, pp.76-77.

Rosen, A., Garme, K., "Slamming Studies on High-Speed Planing Craft through Full-Scale Trials and Simulations",

5th International Conference on Fast Sea Transportation, Seattle, September 1999.

Miles, M.D., "Measurement of six degree of freedom model motions using strapdown accelerometers", 21st ATTC, Washington D.C., 1986, pp369-375.

Det Norske Veritas, "Tentative rules for classification of High Speed and Light Craft", Part 3, Ch.1, January 1991.

American Bureau of Shipping, "Rules for building and classing High Speed Craft", 1997.

Draft ISO Standard 12215 for Small Craft – Hull Construction/Scantling, Part 5, June 2000.

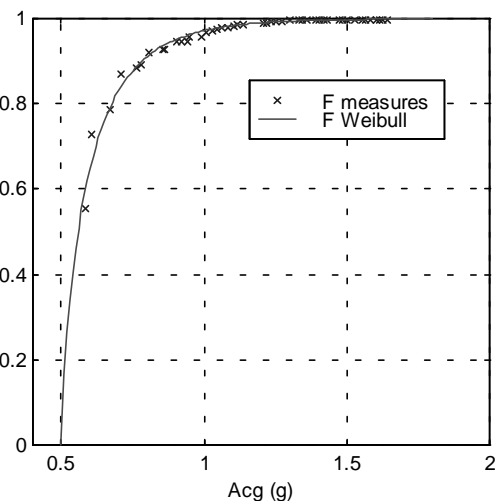
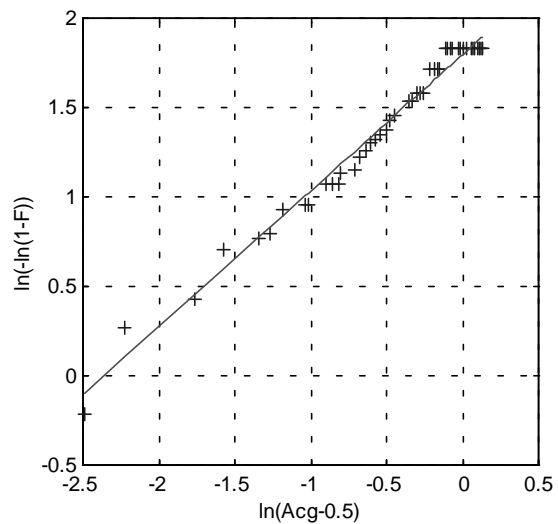


Fig.11 Example of measurements of peak acceleration at the centre of gravity fitting a Weibull probability distribution function.